Synthesis of wavelet basis for analysis of optical signals. Part 2. Biorthogonal and complex wavelet bases

Yu.N. Isaev

Institute of Optical Monitoring,
Siberian Branch of the Russian Academy of Sciences, Tomsk

Received February 3, 2003

An algorithm for synthesis of biorthogonal and complex wavelets is described in detail. Examples of signal restoration and compression based on wavelets constructed are presented. Similarity of these wavelet bases to the Karhunen–Loeve basis is considered. A pattern of spatiotemporal development of a random signal over inhomogeneity scales is presented. Examples of expansion and compression of two-dimensional signals with filtering by directions are presented.

Introduction

In the first part of this paper, the orthogonal wavelet basis for analysis and synthesis of signals was considered.[1] When synthesizing an orthogonal basis, the number of symmetric wavelets at a fixed wavelet carrier is limited. In contrast to synthesis of orthogonal wavelets, synthesis of non-orthogonal wavelets has much more freedom in selection of the shape, smoothness, symmetry, and such important criteria as localization and the number of zero moments, that is, the class of non-orthogonal wavelets is much wider. In this part of the paper, the algorithm for construction of non-orthogonal wavelets similar to the statistically optimal Karhunen–Loeve basis[2] will be considered in detail and the algorithm will be presented for construction of complex wavelets, which are useful in analysis and synthesis of the amplitude and phase of optical complex signals. In conclusion, the processing of two-dimensional signals will be demonstrated.

Theory

When resolving a signal $f(x)$ in a non-orthogonal wavelet basis, it is necessary to have two bases: the wavelet $\Psi(x)$, with respect to which the signal is resolved, and the dual wavelet $\tilde{\Psi}(x)$, which is used to determine the resolution coefficients, that is,

$$f(x)=\sum_{jk}^{N} c_{jk}\Psi_{jk}(x)\,. \qquad (1)$$

Here $\Psi_{jk}(x) = 2^{-j/2}\,\Psi(2^{-j}x - k)$;

$$c_{jk} = \langle f,\ \tilde{\Psi}_{jk}\rangle = \int_{-\infty}^{\infty} f(x)\,\tilde{\Psi}_{jk}(x)\,\mathrm{d}x, \qquad (2)$$

and the following equation is fulfilled:

$$\langle \Psi_{mn},\ \tilde{\Psi}_{jk}\rangle = \delta_{m,j},\ \delta_{n,k}, \qquad (3)$$

where $\delta_{m,j}$ is the Kronecker symbol. The wavelets Ψ and $\tilde{\Psi}$ are called biorthogonal and are formed based on scaling functions φ and $\tilde{\varphi}$, which obey the two-scale equations

$$\varphi(x) = \sum_{k=0}^{N} p_k\,\varphi(2x - k),\ \tilde{\varphi}(x) = \sum_{k=0}^{\tilde{N}} \tilde{p}_k\,\tilde{\varphi}(2x - k). \qquad (4)$$

The upper summation limits N and $\tilde{N}$ are the carriers of the functions φ and $\tilde{\varphi}$, respectively, that is, $N = \mathrm{supp}\ \varphi(x)$ and $\tilde{N} = \mathrm{supp}\ \tilde{\varphi}(x)$. After the coefficients p_k and $\tilde{p}_k$ are determined from Eqs. (4), it is possible to find Ψ and $\tilde{\Psi}$ as

$$\Psi(x) = \sum_{k=0}^{\tilde{N}} (-1)^{k+1}\,\tilde{p}_{-k+1}\varphi(2x - k),$$

$$\tilde{\Psi}(x) = \sum_{k=0}^{N} (-1)^{k+1}\tilde{p}_{-k+1}\,\tilde{\varphi}(2x - k). \qquad (5)$$

Thus, to find the wavelets Ψ and $\tilde{\Psi}$, it is necessary to determine the coefficients p_k and $\tilde{p}_k$ in Eqs. (4). To do this, write the resolutions (4) in the frequency region

$$\hat{\varphi}(\kappa) = \hat{\varphi}(\kappa/2)\,\frac{1}{2}\sum_{k=0}^{N} p_k\,\exp(-jk\kappa/2),$$

$$\hat{\tilde{\varphi}}(\kappa) = \hat{\tilde{\varphi}}(\kappa/2)\,\frac{1}{2}\sum_{k=0}^{\tilde{N}} \tilde{p}_k\,\exp(-jk\kappa/2), \qquad (6)$$

where

$$\hat{\varphi}(\kappa) = \frac{1}{2\pi}\int_{-\infty}^{\infty} \varphi(x)\,\exp(-jx\kappa)\,\mathrm{d}x,$$

and introduce designations for filters

0235-6880/03/04 299-09 $02.00

$$m(\kappa) = \frac{1}{2}\sum_{k=0}^{N} p_k \exp(-jk\kappa/2),$$
$$\tilde{m}(\kappa) = \frac{1}{2}\sum_{k=0}^{N} \tilde{p}_k \exp(-jk\kappa/2). \quad (7)$$

Fulfillment of the orthogonality condition (3) for Ψ and $\tilde{\Psi}$ is equivalent to fulfillment of the following conditions for filters[3,4]:

$$m(\kappa)\,\bar{\tilde{m}}(\kappa) + m(\kappa+\pi)\,\bar{\tilde{m}}(\kappa+\pi) = 1. \quad (8)$$

The overbar denotes a complex conjugation.

If $m(\kappa)$ is taken as a filter, then, solving Eq. (8), we can find $\tilde{m}(\kappa)$. Before explaining how to solve Eq. (8), let us digress for a moment. In Introduction, it was stated that, when compressing an image, it is desirable to have wavelets with a large number of zero moments. Explain this briefly. Let a signal $f(x)$ be expanded into a series

$$f(x) = \sum_{jk}^{N} c_{jk}\, 2^{-j/2}\, \Psi(2^{-j}x - k). \quad (9)$$

If we expand the signal $f(x)$ into the Taylor series in the vicinity of the point k, then we can obtain

$$f(x) = f(k) + f'(k)(x-k) + \frac{1}{2}f''(x-k)^2 + \ldots + \frac{1}{n!}f^{(n)}(x-k)^n + \ldots . \quad (10)$$

If we multiply this equation by $\tilde{\Psi}(2^{-j}x - k)$ and integrate, then, the terms, for which the relation

$$\int \tilde{\Psi}(x)\, x^n\, dx = 0 \quad (11)$$

is fulfilled, will be apparently removed from the series. The terms of the higher order of smallness in Eq. (10) are negligibly small. During signal compression, the coefficients (significant) are sorted above some threshold value. Obviously, the larger is the number of zero moments, the better is the signal compression, that is, the smaller is the number of coefficients for signal presentation. In this sense, the symmetric wavelet basis is close to the optimal Karhunen–Loeve basis.[2] The similarity shows itself in the fact that the Karhunen–Loeve basis has some uncorrelated coefficients, while the wavelet basis has weakly correlated expansion coefficients, and this is a criterion of good compression. Weak correlation of the wavelet basis is explained by the fact that carriers of basis functions (closing of sets, in which functions are nonzero) are spatially (or temporally) separated. Coming back to Eq. (8), it should be noted that it allows one to synthesize wavelets with any number of zero moments. Present the algorithm for synthesis of a wavelet with the needed number of zero moments.

To construct the wavelets Ψ and $\tilde{\Psi}$ means to find $m(\kappa)$ and $\tilde{m}(\kappa)$. Select $m(\kappa)$ in the form

$$m(\kappa) = \cos^n(\kappa/2)\, P[\sin^2(\kappa/2)], \quad (12)$$

if n is even, and in the form

$$m(\kappa) = \exp(j\kappa/2)\cos^n(\kappa/2) P[\sin^2(\kappa/2)], \quad (13)$$

if n is odd. In this equation, n is the power of the first term $\cos^n(\frac{1}{2}\kappa)$; it determines the number of zero moments in the wavelet under construction,[3,4] and $P(x)$ is some polynomial. With the form of $m(\kappa)$ selected, we will find the solution for $\tilde{m}(\kappa)$ in the form

$$\tilde{m}(\kappa) = \cos^s(\kappa/2)\, \tilde{P}[\sin^2(\kappa/2)], \quad (14)$$

if n is even, and in the form

$$\tilde{m}(\kappa) = \exp(j\kappa/2)\cos^s(\kappa/2)\, \tilde{P}[\sin^2(\kappa/2)], \quad (15)$$

if n is odd.

Introduce the following designations $x = \sin^2(\kappa/2)$ and $(1-x)^{s/2}\,\tilde{P}(x) = \tilde{m}(\kappa)$ and substitute Eq. (12) or (13) and, respectively, Eq. (14) or (13) into Eq. (8). As a result, we obtain the Bezout equation[5]:

$$(x-1)^N B(x) + x^N B(1-x) = 1,$$

where $B(x) = \tilde{P}(x)\,P(x)$; $N = (s+n)/2$. The general solution of the Bezout equation has the following form:

$$B(x) = \sum_{k=0}^{N-1} C(N+k-1,\, k)\, x^k + x^N f(x - 1/2), \quad (16)$$

where $C(N,k)$ is the number of combinations of k of n elements; $f(x)$ is any odd function. The first and second terms of Eq. (16) are the particular and general solutions of the inhomogeneous Bezout equation, respectively. Taking different N and $f(x)$ at the selected $m(\kappa)$, in accordance with Eq. (16), we obtain a quite certain equation for $\tilde{m}(\kappa)$. Present a specific example for even and odd N. Selecting $N = 3$ and $f(x) = x + x^3$, we have

$$B(x) = 1 + 3x + 6x^2 + x^3[x - 1/2 + (x - 1/2)^3]. \quad (17)$$

Determine the roots of Eq. (17) and write it in the factorized form

$$B(x) = A\prod_{j=1}^{3}(x^2 - 2\mathrm{Re}(z_j) + |z_j|^2), \quad (18)$$

where A is a constant, which can be easily found by dividing Eq. (17) by Eq. (18); in our case $A = 1$; $z_j = \mathrm{Re}(z_j) + j\mathrm{Im}(z_j)$ are three pairs of complex conjugate roots:

$$z_1 = -0.4763090739 - j1.2303119751,\ \bar{z}_2 = z_1,$$
$$z_3 = -0.2533865279 - j0.30248926121,\ \bar{z}_4 = z_3,$$
$$z_5 = -1.47969571803 - j1.22491119812,\ \bar{z}_6 = z_5.$$

Then select

$$P(x) = (x^2 - 2\mathrm{Re}(z_2) + |z_2|^2),\ n = 5, \quad (19)$$

$$m(\kappa) = \exp(j\kappa/2)\cos^5(\kappa/2)\,P\,[\sin^2(\kappa/2)], \quad (20)$$

then $\tilde{m}(\kappa)$ can have the unique form

$$\tilde{P}(x) = (x^2 - 2\mathrm{Re}(z_1) + |z_1|^2) \times$$
$$\times\,(x^2 - 2\mathrm{Re}(z_3) + |z_3|^2),\ s = 1, \quad (21)$$

$$\tilde{m}(\kappa) = \exp(j\kappa/2)\cos(\kappa/2)\,\tilde{P}\,[\sin^2(\kappa/2)]. \quad (22)$$

Expand $m(\kappa)$ and $\tilde{m}(\kappa)$ into the Fourier series (7) and obtain ten coefficients p_k and ten $\tilde{p}_k$ for the scaling function $\varphi(x)$ (Fig. 1*a*) and the dual function $\tilde{\varphi}(x)$ (Fig. 1*b*), respectively. Expansion into the Fourier series can be obtained by using the trigonometric formulae

$$\cos^n(x) = \left(\frac{e^{jx} + e^{-jx}}{2}\right)^n,\ \sin^n(x) = \left(\frac{e^{jx} - e^{-jx}}{2j}\right)^n,$$

but it is much easier to perform Fourier series expansion in the Mathcad environment. Then, following the algorithm described in the first part of this paper,[1] we can construct the scaling function and the corresponding wavelets. The wavelets Ψ and $\tilde{\Psi}$, as well as their scaling functions are plotted in Figs. 1*a* and *b*. To construct the next pair of wavelets, $n = 3$ in Eq. (19) and $s = 3$ in Eq. (21) should be taken. In this case, expanding $m(\kappa)$ and $\tilde{m}(\kappa)$ into the Fourier series (7), we obtain twelve coefficients p_k and ten coefficients $\tilde{p}_k$. The scaling functions and wavelets corresponding to these coefficients are depicted in Figs. 1*c* and *d*. If we take $n = 5$, $s = 1$ and move the root z_1 from Eq. (21) into Eq. (19), then we obtain the coefficients and the corresponding scaling functions plotted in Figs. 1*e* and *f*.

Dwell now on the example for even $N = 4$. In this case, the solution of the Bezout equation will look as:

$$B(x) = 1 + 4x + 10x^2 + 20x^3 + x^4\,f(x - 1/2). \quad (23)$$

Take the odd function $f(x) = x + x^3$ as $f(x)$. Find the roots $B(x)$ and write them in the factorized form

$$B(x) = A(x - x_0)\prod_{j=1}^{3}(x^2 - 2\mathrm{Re}(z_j) + |z_j|^2). \quad (24)$$

In this case, we obtain one real root $x_0 = -0.3378926514$ and three pairs of complex conjugate roots $z_j = \mathrm{Re}(z_j) + j\mathrm{Im}(z_j)$:

$$z_1 = -0.9055499544 - j1.581306455,\ \bar{z}_2 = z_1,$$
$$z_3 = -8.1141156107\cdot10^{-2} - j0.3725006021,\ \bar{z}_4 = z_3,$$
$$z_5 = 1.9056374362 - j1.5814099917,\ \bar{z}_6 = z_5.$$

Now we can write the equations for $m(\kappa)$ and $\tilde{m}(\kappa)$ in the form (12) and (14), respectively, where $P(x)$ and $\tilde{P}(x)$ are different combinations of factors of Eq. (24). Expanding the filters $m(\kappa)$ and $\tilde{m}(\kappa)$ into the Fourier series, we obtain the coefficients p_k and $\tilde{p}_k$. Some possible versions of solutions for even and odd N are shown in Fig. 2.

Note that at fixed N the class of possible solutions can be extended by changing the form of the function $f(x)$, but the carriers of the wavelet and its scaling function in this case increase.

Consider then resolution of a signal in the bases obtained. Figure 3 depicts the model signal (Fig. 3*a*) and its wavelet resolution (Figs. 3*b–d*).

The wavelets shown in Fig. 1*a* (the number of zero moments $s = 3$) and Fig. 2*d* ($s = 6$) are taken as a basis. Figures 3*b* and *c* illustrate restoration of a signal with compression for the wavelet with $s = 6$; Fig. 3*b* corresponds to 32 coefficients of 256, and Fig. 3*c* – to 128 coefficients of 256.

Figures 3*d* and *e* show the same, but for the wavelet with $s = 3$. As would be expected, a better signal compression and restoration (and, consequently, a smaller number of coefficients in the series) were needed for the wavelet with a larger number of zero moments $s = 6$.

For the wavelets obtained, I have checked the criterion of localization, which is expressed as

$$\Delta x\,\Delta\kappa \geq \frac{1}{2}, \quad (25)$$

where

$$\Delta x = \frac{\int|\Psi(x)|^2(x - x_0)^2\mathrm{d}x}{\int|\Psi(x)|^2\mathrm{d}x},$$

$$\Delta\kappa = \frac{\int|\hat{\Psi}(\kappa)|^2(\kappa - \kappa_0)^2\mathrm{d}\kappa}{\int|\hat{\Psi}(\kappa)|^2\mathrm{d}\kappa}. \quad (26)$$

As the number of zero wavelet moments increases, the inequality (25) fast tends to the equality. That is, wavelets are modulated by the Gaussian function, so they approach the eigenfunctions of the Fourier operator[6] and become optimal by the criterion (25). This means that the signal of a limited length with a fixed number of the terms in the series has the highest energy, if it is presented by the wavelet basis meeting the equality (25), and this is one more similarity to the Karhunen–Loeve basis. With such wavelets, it is convenient to search the hidden periodicity in signals under study and to determine their multifractal structure.

Consider the wavelet resolution of a random signal – the wind velocity shown at the top of Fig. 3*f* – with the wavelet shown in Fig. 2*c* as a basis.

Absolute values of coefficients of wavelet resolution of the random signal (wind velocity) are shown at the bottom of Fig. 3*f*. This pattern demonstrates relative contribution of different-scale inhomogeneities to formation of a signal.

$p_0 = p_9 = 0.0004301$
$p_1 = p_8 = 0.0004417$
$p_2 = p_7 = 0.009309$
$p_3 = p_6 = 0.0101488$
$p_4 = p_5 = 0.6867772$

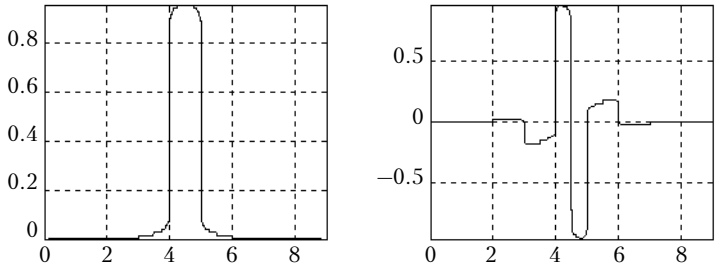

a

$\tilde{p}_0 = \tilde{p}_9 = 0.0177396$
$\tilde{p}_1 = \tilde{p}_8 = 0.0182202$
$\tilde{p}_2 = \tilde{p}_7 = -0.1346437$
$\tilde{p}_3 = \tilde{p}_6 = -0.1140526$
$\tilde{p}_4 = \tilde{p}_5 = 0.7281784$

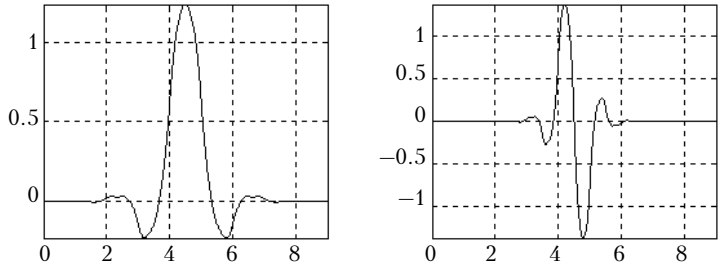

b

$p_0 = p_{11} = 0.0004301$
$p_1 = p_{10} = 0.0004417$
$p_2 = p_9 = 0.009309$
$p_3 = p_8 = 0.0101488$
$p_4 = p_7 = 0.6867772$
$p_5 = p_6 = 0.6867772$

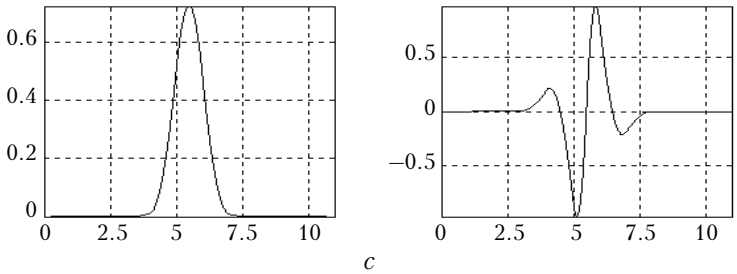

c

$\tilde{p}_0 = \tilde{p}_9 = 0.0177396$
$\tilde{p}_1 = \tilde{p}_8 = 0.0182202$
$\tilde{p}_2 = \tilde{p}_7 = -0.1346437$
$\tilde{p}_3 = \tilde{p}_6 = -0.1140526$
$\tilde{p}_4 = \tilde{p}_5 = 0.7281784$

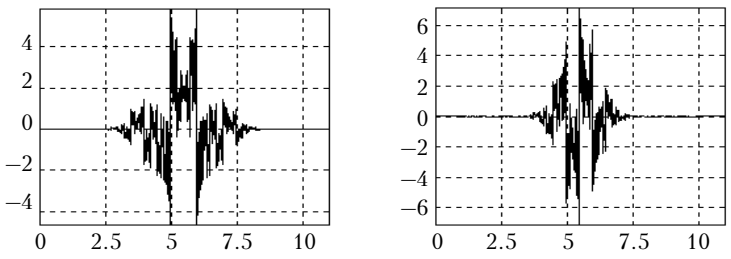

d

$p_0 = p_5 = 0.011997$
$p_1 = p_4 = 0.1058479$
$p_2 = p_3 = 0.5892818$

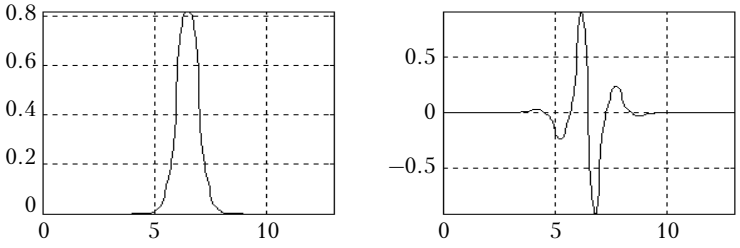

e

$\tilde{p}_0 = \tilde{p}_{13} = 0.000637$
$\tilde{p}_1 = \tilde{p}_{12} = -0.0056295$
$\tilde{p}_2 = \tilde{p}_{11} = 0.0266914$
$\tilde{p}_3 = \tilde{p}_{10} = 0.0097508$
$\tilde{p}_4 = \tilde{p}_9 = -0.2005914$
$\tilde{p}_5 = \tilde{p}_8 = 0.0288662$
$\tilde{p}_6 = \tilde{p}_7 = 0.843824$

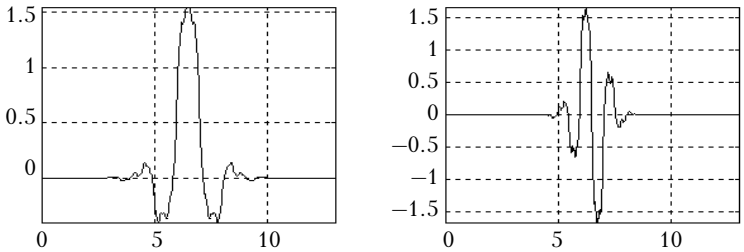

f

Fig. 1.

$p_0 = p_{16} = -0.00013233$
$p_1 = p_{15} = 0.00175273$
$p_2 = p_{14} = -0.01181917$
$p_3 = p_{13} = 0.00878867$
$p_4 = p_{12} = 0.08313578$
$p_5 = p_{11} = -0.11690713$
$p_6 = p_{10} = -0.29571447$
$p_7 = p_9 = 0.45991912$
$p_8 = 1.15616716$

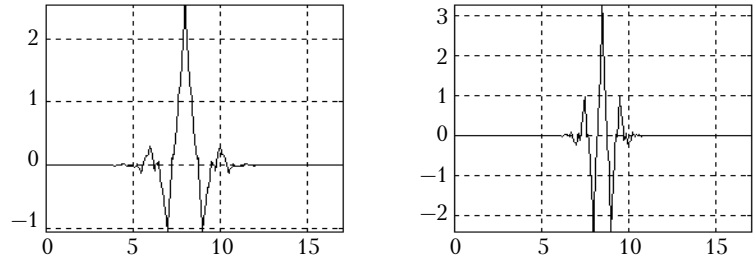

a

$\tilde{p}_0 = \tilde{p}_6 = 0.00360339$
$\tilde{p}_1 = \tilde{p}_5 = 0.04772721$
$\tilde{p}_2 = \tilde{p}_4 = 0.34995$
$\tilde{p}_3 = 0.61165236$

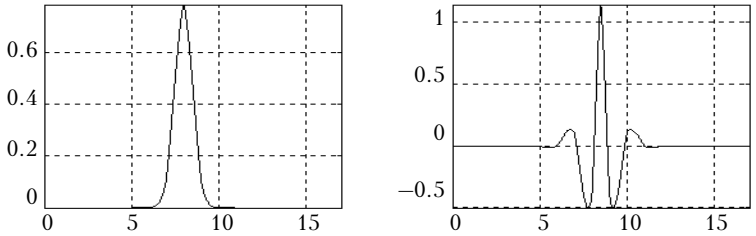

b

$p_0 = p_{18} = -0.00136135$
$p_1 = p_{17} = 0.0054454$
$p_2 = p_{16} = 0.00468923$
$p_3 = p_{15} = -0.04598393$
$p_4 = p_{14} = 0.01771813$
$p_5 = p_{13} = 0.18082888$
$p_6 = p_{12} = -0.15619841$
$p_7 = p_{11} = -0.48524242$
$p_8 = p_{10} = 0.48870579$
$p_9 = 1.39701094$

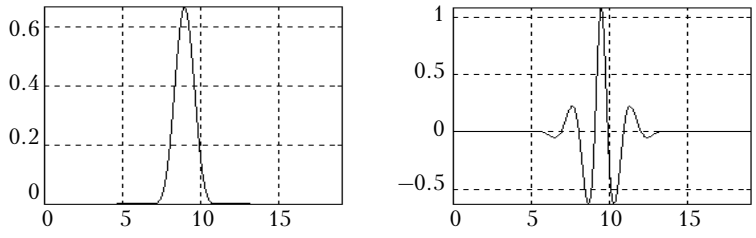

c

$\tilde{p}_0 = \tilde{p}_{10} = 0.00000137$
$\tilde{p}_1 = \tilde{p}_9 = 0.00000547$
$\tilde{p}_2 = \tilde{p}_8 = 0.00003618$
$\tilde{p}_3 = \tilde{p}_7 = 0.08849887$
$\tilde{p}_4 = \tilde{p}_6 = 0.35343055$
$\tilde{p}_5 = 0.53003394$

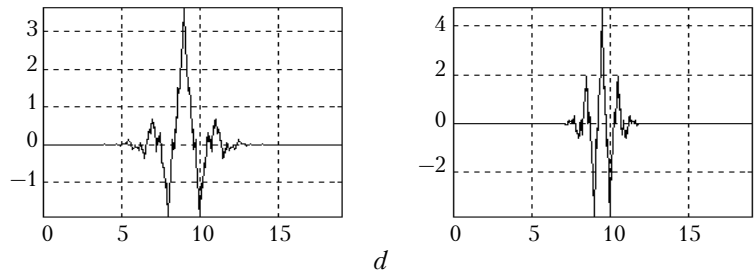

d

$p_0 = p_{16} = -0.00002804$
$p_1 = p_{15} = -0.00060931$
$p_2 = p_{14} = 0.00674686$
$p_3 = p_{13} = 0.00592045$
$p_4 = p_{12} = 0.03761214$
$p_5 = p_{11} = -0.02871934$
$p_6 = p_{10} = -0.03011743$
$p_7 = p_9 = 0.37696159$
$p_8 = 0.70566718$

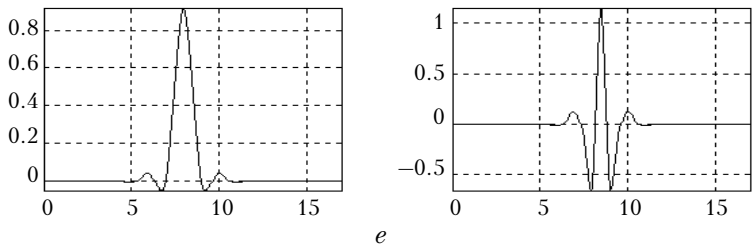

e

$\tilde{p}_0 = \tilde{p}_{14} = 0.00006642$
$\tilde{p}_1 = \tilde{p}_{13} = -0.00144319$
$\tilde{p}_2 = \tilde{p}_{12} = 0.01584165$
$\tilde{p}_3 = \tilde{p}_{11} = 0.01703875$
$\tilde{p}_4 = \tilde{p}_{10} = -0.121698$
$\tilde{p}_5 = \tilde{p}_9 = -0.11432698$
$\tilde{p}_6 = \tilde{p}_8 = 0.45934331$
$\tilde{p}_7 = 0.90456961$

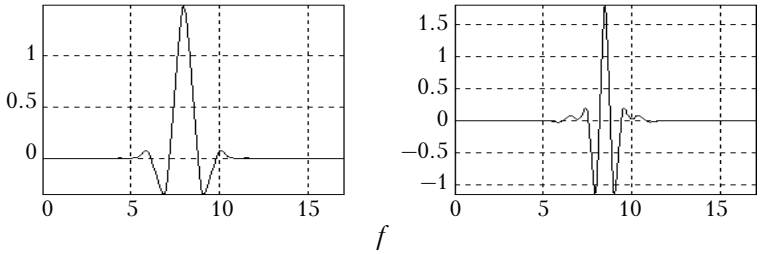

f

Fig. 2.

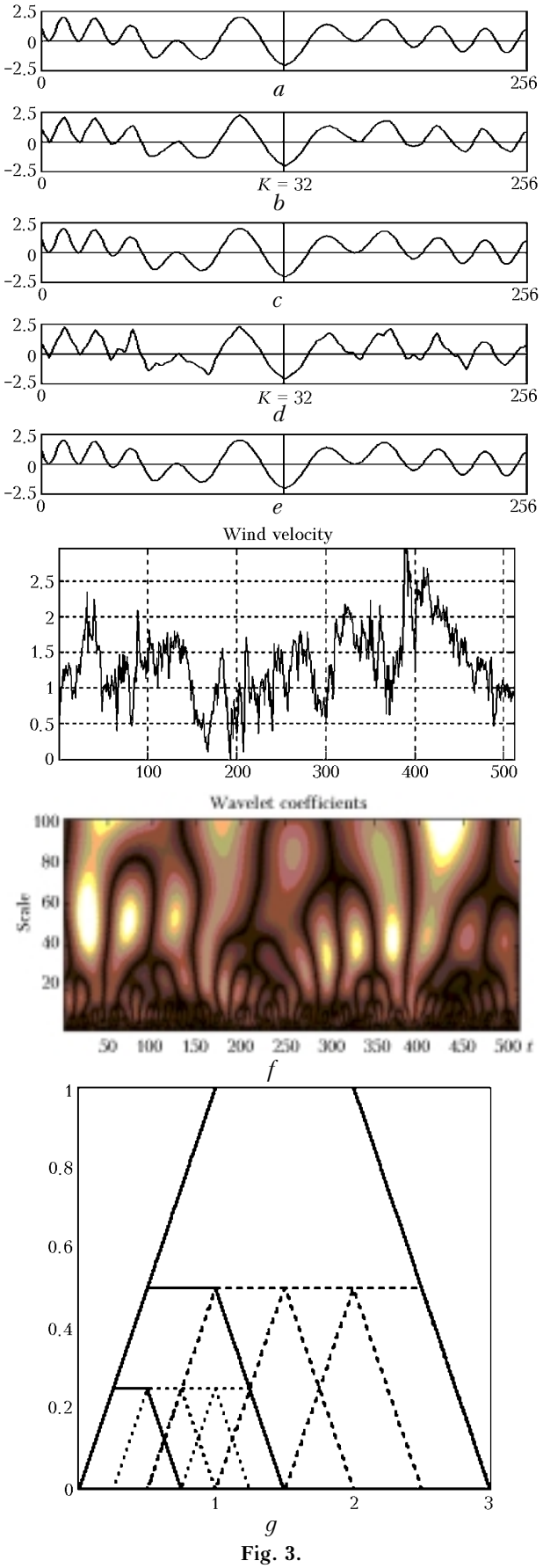

Fig. 3.

It can be seen from the figure that large-scale inhomogeneities break into smaller ones, which, in their turn, also break into even smaller ones, and this cascade process continues up to the smallest fraction of inhomogeneities, as indicated by the characteristic branching — "forks." This example demonstrates a similarity of a random signal to a multifractal structure of the inhomogeneous Cantor series, so the signal propagation medium can be described by a power spectrum of κ^{α} type, if we assume that α is a function of κ. We succeeded in obtaining such a physical pattern of inhomogeneities due to fractal properties of the wavelet scaling functions, that is, Eq. (4), whose meaning is demonstrated graphically in Fig. 3*g*, where for simplicity the trapezoidal function is taken as a scaling function:

$$\varphi(x) = \frac{1}{2}\,\varphi(2x) + \frac{1}{2}\,\varphi(2x-1) + \frac{1}{2}\,\varphi(2x-2) + \frac{1}{2}\,\varphi(2x-3). \qquad (27)$$

Each trapezium consists of four similar trapeziums, and this cascade process (resembling the process of interaction between vortices in a turbulent process) can be infinitely continued in the both directions: to increase or decrease of the trapezium dimensions. It can be easily noticed that this basis more adequately corresponds to the structure of a turbulent flow and, consequently, more adequately describes it.

In some cases, it is convenient to analyze the amplitude and phase of an optical signal in its complex presentation. In this case, complex wavelets are convenient for resolution. The scaling function $\varphi(x)$ in this case has complex coefficients, and the dual function is the conjugate function

$$\tilde{\varphi}(x) = \overline{\varphi}(x). \qquad (28)$$

Let us present the algorithm for synthesis of complex wavelets. Given is the real part of coefficients in Eq. (4), whose sum is equal to unity, for example

$$\mathrm{Re}(p_0) = \mathrm{Re}(p_1) = \mathrm{Re}(p_2) = \mathrm{Re}(p_3) = \frac{1}{4}\,. \qquad (29)$$

Then we find the imaginary part of the coefficients $\mathrm{Im}(p_k)$ from the equation of orthogonality (8) with allowance for the condition (28)

$$p_0 = p_3 = \frac{1}{4} + j\,\frac{1}{4}\,, \quad p_1 = p_2 = \frac{1}{4} - j\,\frac{1}{4}\,. \qquad (30)$$

After determination of the coefficients, find the scaling and wavelet functions using Eqs. (4) and (5), respectively. Complex wavelets can be obtained in the same way, using the complex solution of the Bezout equation. For example, at $N = 3$ the solution can be written in the form

$$B(x) = A \prod_{j=1}^{3} (x - z_j)\,(x - \overline{z}_j), \qquad (31)$$

then the equations for the filters $m(\kappa)$ and $\tilde{m}(\kappa)$ will include various combinations of complex factors from Eq. (31). Figure 4 depicts the wavelets obtained by the algorithm described.

$P_0 = 0.003536 - j\ 0.049875$
$p_1 = 0.703571 + j\ 0.049875$
$p_2 = 0.703571 + j\ 0.049875$
$p_3 = 0.003536 - j\ 0.049875$

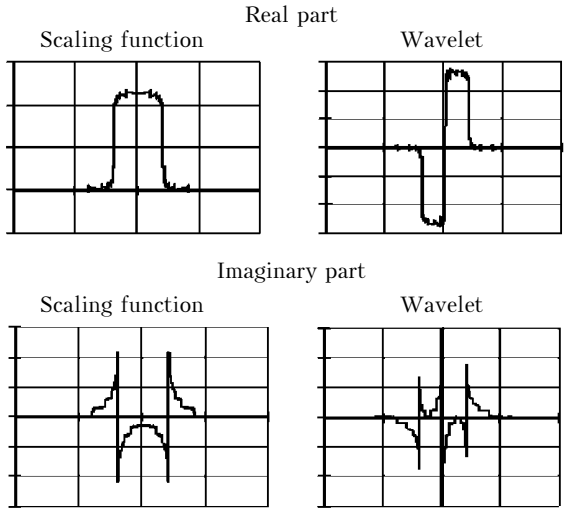

a

$p_0 = 0.25 - j\ 0.25$
$p_1 = 0.25 + j\ 0.25$
$p_2 = 0.25 + j\ 0.25$
$p_3 = 0.25 - j\ 0.25$

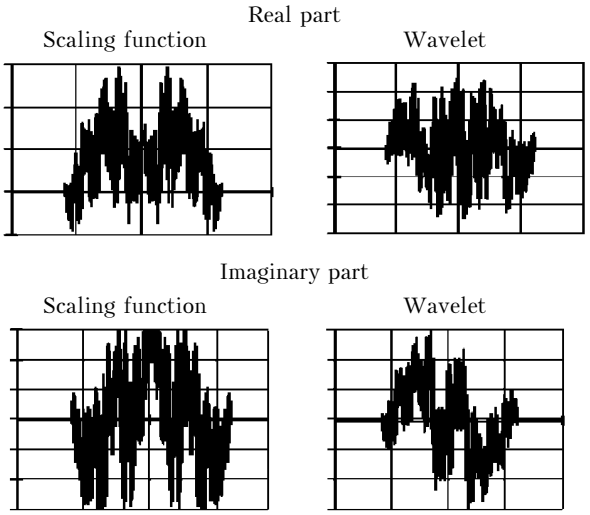

b

$p_0 = -0.0785674 - j\ 0.1111111$
$p_1 = 0.1571348 - j\ 0.1111111$
$p_2 = 0.6285394 + j\ 0.222222$
$p_3 = 0.6285394 + j\ 0.222222$
$p_4 = 0.1571348 - j\ 0.1111111$
$p_5 = -0.0785674 - j\ 0.1111111$

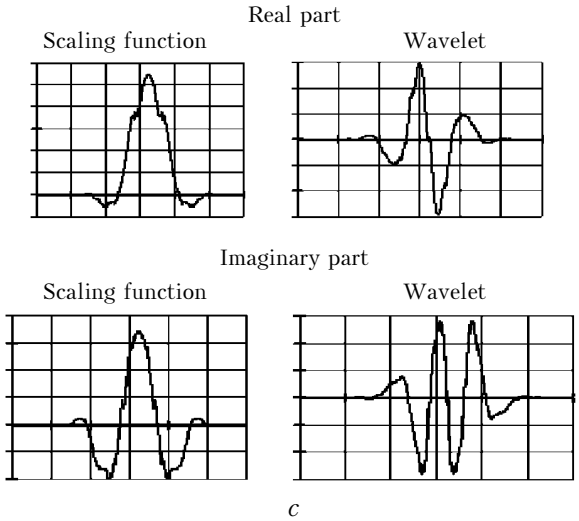

c

Fig. 4.

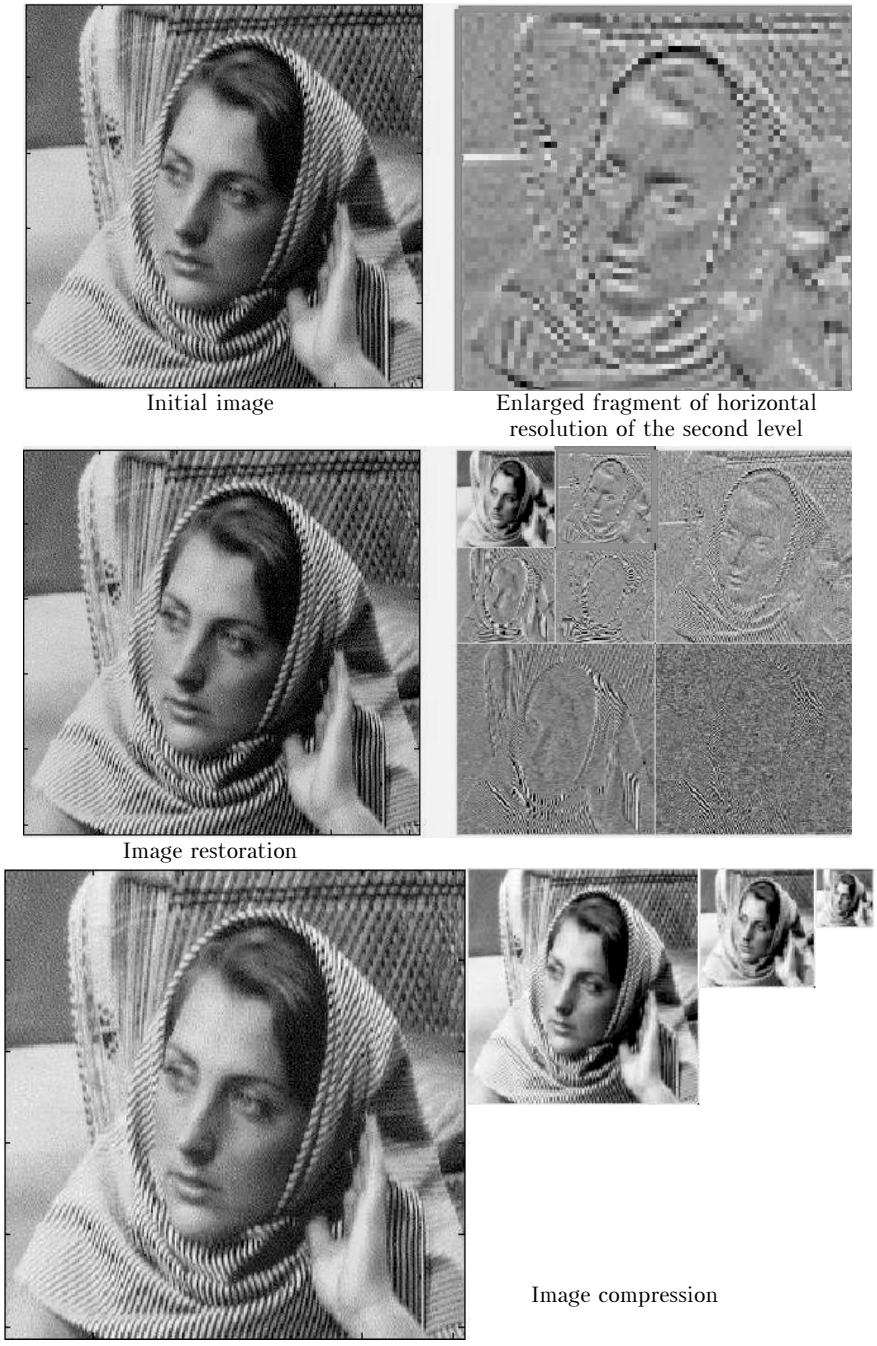

Fig. 5.

Present an example of using the wavelet basis for processing two-dimensional images. Having written the tensor product of one-dimensional wavelets, we get the equations for three two-dimensional wavelets

$$\Psi^{h}(x,y) = \varphi(x)\,\Psi(y), \quad \Psi^{v}(x,y) = \Psi(x)\,\varphi(y),$$
$$\Psi^{d}(x,y) = \varphi(x)\varphi(y). \qquad (32)$$

This representation is convenient, because the image is filtered in the horizontal, vertical, and diagonal directions, and the corresponding wavelets are marked by the superscripts. Through shifts and compression, we obtain the basis

$$\Psi_{j,n1,n2}(x,y) = 2^{-j}\,\Psi(2^{-j}x - n1,\ 2^{-j}y - n2). \qquad (33)$$

All equations (1)–(5) presented for the one-dimensional case remain correct for the two-dimensional basis. The wavelets presented here and in Ref. 1 were obtained in the Wavelet Toolbox GUI (MATLAB 6.1), which significantly facilitates the use of wavelets for synthesis and analysis of two-dimensional images. As an example of Wavelet Toolbox operation, Figure 5 (bottom) presents an

example of compression of a 2-D image with the wavelet shown in Fig. 2*b*. The initial number of the coefficients was 256 × 256 and then it was halved. To separate the edge effects in the image with allowance for the direction, take the wavelet shown in Fig. 6*b* from Ref. 1. The results of reconstruction shown in Fig. 5 (top) clearly demonstrate the useful property of wavelets to filter by directions.

Conclusion

This paper presents the groups of new biorthogonal and complex wavelets, as well as the algorithm for their synthesis, along with the examples of synthesis and analysis of model signals. It is shown possible to visualize the fractal structure of the signal and the scales of inhomogeneity of the signal propagation medium using the wavelet resolution coefficients. The useful properties of the obtained wavelets to filter by directions and to separate a fine structure of an image are demonstrated.

Acknowledgments

I would like to express my gratitude to S.V. Loginov for his help in installation of wavelets in the Wavelet Toolbox GUI (MATLAB 6.1), as well as to A.L. Afanas'ev for the experimental data kindly placed at my disposal.

References

1. Yu.N. Isaev, Atmos. Oceanic Opt. **15**, No. 11, 883–890 (2002).
2. Yu.N. Isaev and E.V. Zakharova, Atmos. Oceanic Opt. **11**, No. 5, 393–396 (1998).
3. I. Daubechies, *Ten Lectures on Wavelets* (SIAM, Philadelphia, PA, 1992).
4. C.K. Chui, *An Introduction to Wavelets* (Academic Press, New York, 1992).
5. R.A. De Vore, B. Jawerth, and B.J. Lucier, IEEE Transactions on Information Theory **38**, No. 2, 719–746 (1992).
6. Ya.I. Khurgin and V.P. Yakovlev, *Finite Functions in Physics and Technology* (Nauka, Moscow, 1971), 406 pp.